Journal of Power Sources 293 (2015) 373–379

Contents lists available at ScienceDirect

Journal of Power Sources

journal homepage: www.elsevier.com/locate/jpowsour

Polyaniline-coated freestanding porous carbon nanofibers as efficient hybrid electrodes for supercapacitors

Chau Tran, Richa Singhal, Daniel Lawrence, Vibha Kalra*

Department of Chemical and Biological Engineering, Drexel University, 3141 Chestnut St., Philadelphia, PA 19104, USA

HIGHLIGHTS

- A conformal and uniform coating of polyaniline was electrochemically deposited on porous carbon nanofibers.
- Galvanostatic PANI deposition was found to be the most effective technique.
- Successfully integrated the electric double layer capacitance and pseudocapacitance.
- Excellent specific capacitance of up to 409 F g^{-1} was obtained.

ARTICLE INFO

Article history:
Received 23 February 2015
Received in revised form
5 May 2015
Accepted 15 May 2015
Available online

Keywords:
Supercapacitors
Carbon nanofibers
Freestanding
Polyaniline
EDLC/pseudocapacitor hybrid electrodes

ABSTRACT

Three-dimensional, free-standing, hybrid supercapacitor electrodes combining polyaniline (PANI) and porous carbon nanofibers (P-CNFs) were fabricated with the aim to integrate the benefits of both electric double layer capacitors (high power, cyclability) and pseudocapacitors (high energy density). A systematic investigation of three different electropolymerization techniques, namely, potentiodynamic, potentiostatic, and galvanostatic, for electrodeposition of PANI on freestanding carbon nanofiber mats was conducted. It was found that the galvanostatic method, where the current density is kept constant and can be easily controlled facilitates conformal and uniform coating of PANI on three-dimensional carbon nanofiber substrates. The electrochemical tests indicated that the PANI-coated P-CNFs exhibit excellent specific capacitance of 366 F g^{-1} (vs. 140 F g^{-1} for uncoated porous carbon nanofibers), 140 F cm^{-3} volumetric capacitance, and up to 2.3 F cm^{-2} areal capacitance at 100 mV s^{-1} scan rate. Such excellent performance is attributed to a thin and conformal coating of PANI achieved using the galvanostatic electrodeposition technique, which not only provides pseudocapacitance with high rate capability, but also retains the double-layer capacitance of the underlying P-CNFs.

1. Introduction

Polyaniline (PANI) has been considered as a promising pseudocapacitive material due to its high theoretical specific capacitance, low cost, high conductivity, and ease of synthesis. It has a theoretical capacitance of 750 F g^{-1} with the assumption of 0.5 dopant per polymer unit and 0.7 V potential window [1]. Nanostructured PANI has been shown to provide high capacitance and good cyclability [2–6] compared to thicker PANI films, which suffer from inefficient utilization at high power [7,8]. The composites of carbon/conducting polymer combining the superior pseudocapacitance of conducting polymer and stability of the carbon have been shown to exhibit excellent supercapacitive performance [9–12]. PANI nanowires on carbon fiber cloth were shown to exhibit a high area-normalized capacitance of 1.8 F cm^{-2} and a gravimetric capacitance of 1079 F g_{PANI}^{-1} [3]. Another study reported that nanostructured PANI on porous carbon monolith exhibited a specific capacitance of 1580 F g^{-1} with respect to the weight of PANI only and 300 F g^{-1} with respect to the total composite weight [13]. The reported values are, however, higher than PANI's theoretical capacitance of 750 F g^{-1}. Such discrepancy is possibly due to the over-estimation of the material's performance resulting from the small mass of electrodes used during electrochemical characterizations. Moreover, these composites are often impractical for commercialization due to either complicated fabrication methodologies, or insignificant capacitive contribution from the carbon substrate resulting in significant dead mass and lower composite

* Corresponding author.
E-mail address: vk99@drexel.edu (V. Kalra).

http://dx.doi.org/10.1016/j.jpowsour.2015.05.054
0378-7753/

performance [14]. In addition, most works in the past synthesized powder-based electrodes, which need to be blended with insulating binders to form electrodes [2,6,8].

Electrodeposition of PANI is the preferred methodology of PANI deposition over chemical techniques, as the former has been shown to exhibit higher specific capacitance than chemically formed PANI [1]. It is also posited that electrodeposition produces films with superior adhesion and smoothness [15,16]. Several reports have investigated the effect of PANI electrodeposition on planar substrates, e.g., platinum [17] and stainless steel [18]. Overall, these authors concluded that the potentiodynamic technique produces a more uniform PANI film due to periodic interruptions during polymerization between consecutive sweeps. This conclusion was also confirmed by Bleda-Matinez and co-workers [19] when electrodepositing PANI on high surface area–activated carbon. However, they preferred the potentiostatic method as it allowed the formation of a more porous PANI film that resulted in higher capacitance. Contrary to the studies on planar substrates, most reports on electrodeposition of PANI on 3-D carbon substrates select a method without any clear reasoning. For example, few reports chose potentiodynamic method for activated carbon nanofibers [20], carbon nanotube array [21], and multi-walled carbon nanotube coated carbon paper [22], while others chose potentiostatic and pulse potentiostatic techniques for graphene paper [7] and carbon cloth [23] respectively. Some studies also combined potentiodynamic or potentiostatic techniques for initial nucleation followed by galvanostatic for a slow PANI deposition on carbon cloth [24,25]. Also, these reports often show distorted/resistive cyclic voltammetry curves (CVs) at a scan rate of 100 mV s^{-1} indicative of low power handling capability, a property, which, we believe, is directly correlated to the morphology of the coated PANI.

To the best of our knowledge, there are no systematic studies on PANI electropolymerization on three-dimensional (3-D) electrodes/substrates that demonstrate the effect of the technique used on PANI morphology and capacitive performance. In this work, we provide a systematic comparison of three electrodeposition techniques, namely, potentiodynamic, potentiostatic and galvanostatic, on freestanding mats of non-porous (NP-CNF) and porous carbon nanofibers (P-CNF). The non-porous carbon nanofibers serve as the control substrate to compare various PANI electrodeposition techniques without the added complication of porosity in the fiber affecting the nucleation and growth of the electrodeposited polymer. Our past work [26,27] on freestanding porous carbon nanofibers (P-CNFs) showed near-ideal double-layer capacitive behavior at both slow and fast scan rates (up to 2 V s^{-1}) with a specific capacitance of up to 180 F g^{-1} owing to the presence of a hierarchical pore structure in these carbon electrodes. In the present work, we demonstrate that the conformal growth of nanostructured PANI on P-CNFs offers a combination of both double-layer capacitance (porous carbon) and pseudocapacitance (PANI), thus, minimizing dead substrate mass and enhancing composite performance. The conformal and thin coating of PANI provides a closer contact between PANI and carbon, where porous carbon acts as a support that helps PANI to sustain strains during the charge/discharge cycling process, thereby, providing a high rate operation [9].

2. Experimental

2.1. Fabrication of carbon nanofibers

Porous carbon nanofibers (P-CNFs) were prepared via one-step carbonization methodology without any activation procedures as described in detail elsewhere [26,27]. In brief, 22 wt% of 70/30 (wt/wt) Nafion™/polyacrylonitrile blend was dissolved in N,N-dimethylformamide (DMF) under gentle heating and stirring for 1 h. Nanofibers were electrospun at room temperature with relative humidity below 20%. The flow rate was kept constant at 0.2 mL h^{-1}. The electrospun nanofibers were then stabilized by heating at 280 °C under air flow for 5 h, and carbonized at 1000 °C under inert atmosphere for 1 h. During the heat treatment process, the Nafion™ domains thermally decompose out, and the polyacrylonitrile domains are converted to carbon with an interconnected pore network throughout the entire nanofibers. Nonporous carbon nanofibers (NP-CNFs) were prepared by electrospinning a solution containing 10 wt% of polyacrylonitrile in DMF and heat-treated (stabilized and carbonized) using the same procedure as described above for P-CNFs. The scanning electron microscopy (SEM) and transmission electron microscopy (TEM) images of NP-CNF and P-CNF substrates are provided in Supplementary Fig. S1.

2.2. Polyaniline deposition on carbon nanofibers

As-received aniline (purchased from Alfa Aesar) was dissolved in 1 M H_2SO_4. The NP-CNF and P-CNF mats were punched into 1/2″-diameter freestanding electrodes and used as substrates for deposition. The electrochemical polymerization of PANI on these substrates was carried out using a three-electrode cell with Ag/AgCl as the reference electrode and platinum mesh as the counter electrode. All reported potentials are versus Ag/AgCl. A T-type Swagelok cell was employed as shown in Supplementary Fig. S2. In this setup, a graphite rod of 1/2″ diameter was used as the current collector. A 1/2″-diameter NP-CNF or P-CNF mat (working electrode) was placed between the graphite rod and a porous stopper, and the assembly was compressed to minimize contact resistance. The reference electrode was positioned such that it is sufficiently close to the substrate for lower solution resistance. The solution resistance was kept below 1 Ω before each measurement to provide a consistent voltage reading. Three different electropolymerization techniques have been studied: potentiodynamic, sweeping voltage between −0.1 and 1 V at 20 mV s^{-1}; potentiostatic, applying a constant potential of 0.8 V; and galvanostatic, applying a constant current of 9 mA. The PANI deposited from the three techniques (potentiodynamic, potentiostatic, and galvanostatic) is referred to as PD-PANI, P-PANI, and G-PANI respectively in the text. After deposition, samples were thoroughly washed with deionized water to remove any adsorbed electrolyte and dried at 60 °C for at least 2 h. The weight of dried electrode before and after deposition was used to calculate the weight fraction of PANI in the sample.

2.3. Electrochemical and structural characterization

The fabricated materials were electrochemically tested by using cyclic voltammetry (CV) at various scan rates from 20 mV s^{-1} to 200 mV s^{-1} in the voltage window of −0.1–0.65 V in 1 M H_2SO_4. The electrode loading was at least 5 mg cm^{-2}. The composite capacitance, $C_{PANI/C}$ (F $g^{-1}_{PANI/C}$), was calculated using the following equation:

$$C_{PANI/C} = \frac{1}{2}\frac{Q}{m \times V}$$

$$with\ Q = \frac{\int IdV}{\vartheta}$$

where m, V, and ν represent the mass of composite including the substrate and PANI, voltage window and scan rate, respectively. The

integral was calculated using the *Quick integrate* feature of Echem Analyst software (Gamry). The specific capacitance of polyaniline alone, C_{PANI} ($F\,g^{-1}_{PANI/C}$), was calculated using the following equation:

$$C_{PANI} = \frac{\frac{1}{2}Q - C_{substrate} \times m_{substrate} \times V}{m_{PANI} V}$$

where $C_{substrate}$ and $m_{substrate}$ are respectively the specific capacitance and mass of the substrate used (NP-CNF or P-CNF), and m_{PANI} is the mass of PANI. The external morphology of electrospun nanofiber mats was characterized using scanning electron microscopy (SEM) (Zeiss Supra 50VP). The CV curves of uncoated NP-CNF and P-CNF are shown in Supplementary Fig. S3 indicating a $C_{substrate}$ of 10 F g^{-1} and 140 F g^{-1}, respectively.

3. Results and discussion

To better understand the effect of the nature of the electropolymerization technique on morphology and performance of PANI, the initial studies were conducted on NP-CNF (control) substrates. As discussed in the experimental section, NP-CNF substrate by itself has a very small capacitive contribution. First, potentiodynamic method was applied to carry out PANI electropolymerization using a potential sweep between −0.1 and 1.0 V at a scan rate of 20 mV s^{-1} in a solution containing 0.1 M aniline and 1 M H_2SO_4. As PANI electrodeposits on the surface of NP-CNFs, multiple redox peaks appear (Fig. 1(a)), indicating the complexity of electropolymerization. The broad anodic peak 'E' at 0.84 V represents the oxidation of aniline in the first cycle. This peak disappears in subsequent cycles indicating that polymer growth does not simply consist of a buildup of layers on the carbon surface from the aniline oxidation products [28]. Overall, there are four redox couples (A/A′, B/B′, C/C′, D/D′). These features are similar to previous studies on planar platinum substrates [28,29]. Peaks A and A′ correspond to the conversion between the oxidized emeraldine salt (ES) and reduced leucoemeraldine (LB), while peak D represents the oxidation of polymer to form the di-radial di-cation pernigraniline (PB) and D′ is the corresponding reduction peak. Peak D during deposition is also attributed to the reaction between the pre-formed products (in the first few cycles) and aniline for growth of the polymer [28,29]. However, peak D does not increase with cycling suggesting that little or no PANI was formed during the deposition. Instead, there are well-defined redox peaks, B/B′ and C/C′ that are attributed to the formation of degradation products and that increase significantly with cycling.

After three cycles, the sample was removed and thoroughly washed with DI water. Loose flakes were seen on the fiber mat which washed away with water indicating poor adhesion of the deposited material. When electrochemically tested in aniline-free 1 M H_2SO_4, two reversible redox peaks were observed imposed on a near-rectangular capacitive background (Fig. 1(b)). These redox peaks are located at the potential associated with the presence of degradation by-products, namely, hydroquinone and p-hydroxydiphenylamine [29,30], although some studies have incorrectly assigned these peaks to the conversion between ES and PB [8,10,31]. Although these by-products provide reasonable capacitance via reversible reactions, they are expected to have poor adhesion and leach out with time deteriorating the stability of such devices. Investigations by Duic et al. [30] suggested that the by-product/polymer composition in the final product depends on the monomer-to-radical cation ratio, with higher monomer-to-radical cation ratios favoring polymerization over by-product formation. Parameters such as the initial concentration of aniline, potential limit, and scan rate can affect the monomer-to-radical cation ratio.

The potentiodynamic electropolymerization was then repeated with a higher aniline concentration of 0.5 M and a slightly revised potential sweep (−0.1–0.9 V) to minimize the formation of by-products. The CV curve (Fig. 2(a)) obtained in 1 M H_2SO_4 for the resultant PANI-coated NP-CNF sample (5 cycles; 25% PANI loading) shows well-defined redox peaks (A/A′) corresponding to the transformation of LB to ES, with strong suppression of the by-product peaks (B/B′ and C/C′). The intensities of these two peaks are greatly dependent on monomer-to-radical cation ratios. Higher aniline concentration will increase monomer to radical cation ratio and prevent the coupling reaction between the two radicals. This coupling reaction is known to generate 4-aminodiphenylamine which is further oxidized to produce by-products, hydroquinone and p-hydroxydiphenylamine corresponding to peaks B/B′ and C/C′ respectively. When the monomer concentration is high, the radical will instead react with aniline monomer for polyaniline growth. As a result, peaks B/B′ and C/C′ are suppressed in the case of high aniline concentration. Further increasing the number of cycles during potentiodynamic deposition results in more growth of PANI on the outer layers of NP-CNFs, however, they are easily washed away with water. An average composite specific capacitance of only 177 F g^{-1} was obtained. Moreover, the SEM image (Fig. 2(b)) showed a non-uniform and non-conformal coating of PANI on NP-CNFs.

Electrodeposition of PANI was then investigated using potentiostatic and galvanostatic techniques, where the voltage and current are kept constant, respectively. Based on the results from the potentiodynamic study, all subsequent depositions were carried out in solutions containing 0.5 M aniline and 1 M H_2SO_4 to

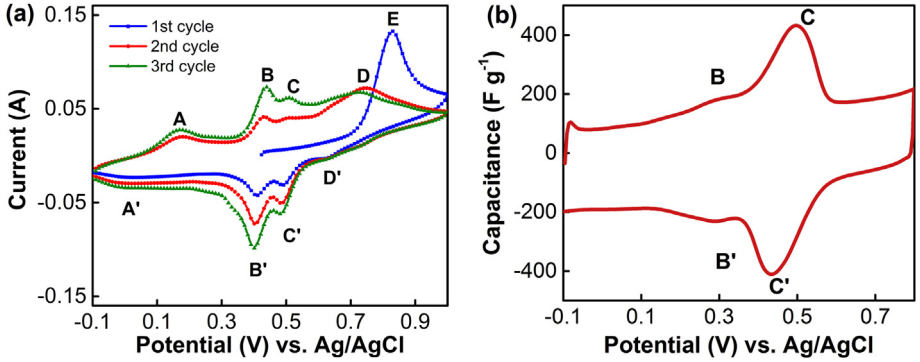

Fig. 1. (a) Voltammetric curves for potentiodynamic electrodeposition on NP-CNF in 0.1 M aniline/1 M H_2SO_4 at a scan rate of 20 mV s^{-1}, (b) corresponding cyclic voltammetric response of PD-PANI-coated NP-CNF at 20 mV s^{-1}.

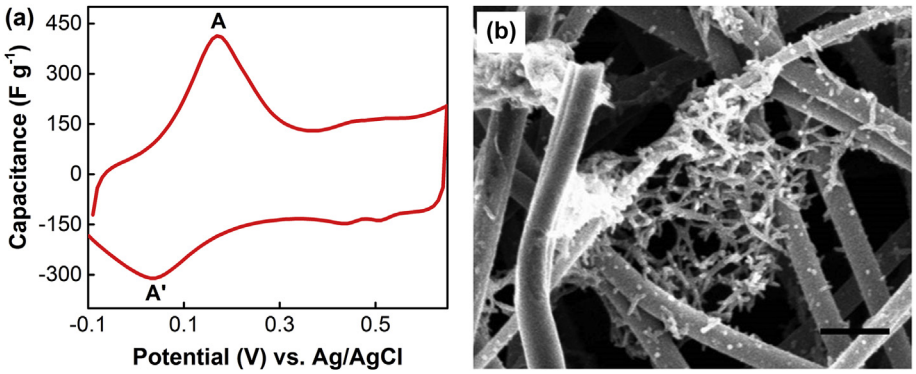

Fig. 2. (a) The cyclic voltammetric response of PD-PANI-coated NP-CNF at 20 mV s^{-1}, where PANI was electrodeposited in 0.5 M aniline/1 M H_2SO_4, (b) corresponding SEM image of PD-PANI-coated NP-CNF. Scale bar = 1 μm.

minimize degradation by-product formation. Previous reports [7,17,19] on the potentiostatic technique have utilized a constant potential in the range of 0.8–1.0 V. For the present study, potentiostatic electropolymerization was carried out at a potential of 0.8 V held constant for 20 s, accumulating a total charge of 2.6 C, which corresponds to 1.03 mg of PANI assuming a consumption of 2.4 electrons per aniline unit. The actual weight of deposited PANI was measured to be 1.0 mg, in good agreement with the calculated value. Fig. 3(a) shows the CV of potentiostatically deposited PANI (P-PANI) on a NP-CNF mat at the scan rate of 20 mV s^{-1}. An average composite specific capacitance of 203.73 F $g^{-1}_{PANI/C}$ was obtained. Assuming a contribution of 10 F g^{-1} from the NP-CNF substrate, the specific capacitance of PANI can be estimated as 570 F g^{-1}_{PANI}. This value is comparable to several earlier studies [7,19]. However, the SEM image (Fig. 3(b)) showed a non-uniform and non-conformal coating of PANI on NP-CNFs, which again is similar to previous works on other carbon-based substrates [13,23,32]. At 0.8 V, a high current of ~150 mA was observed during potentiostatic deposition (with an electrode area of 1.26 cm^2), which was similar to the resultant current during the potentiodynamic coating (Fig. 1(a)). Thus, it was concluded that the high resultant current density in the potentiostatic (as well as potentiodynamic) method results in rapid polymer growth making it difficult to achieve conformal, uniform coating. In addition, the poor adhesion achieved between PANI and NP-CNFs prevents deposition of a higher weight fraction of PANI. We found that deposition time of more than 20 s results in flaky PANI morphology and no enhancement of effective mass (post washing) of the material is obtained.

Galvanostatic electrodeposition of PANI was then studied using 9 mA current, held constant for 600 s. Note that this current is more than an order of magnitude lower than the current achieved during potentiostatic deposition. The difference in the current density is expected to greatly affect the kinetics of electropolymerization and morphology of the deposited PANI (G-PANI). The amount of charge generated during galvanostatic deposition at 9 mA was 5.4 C, which corresponds to about 2.15 mg of deposited PANI assuming the consumption of 2.4 electrons per aniline unit. The weight of deposited PANI was measured to be ~3.0 mg, which is higher than the estimated value. This discrepancy could indicate that the number of electrons consumed per unit aniline during galvanostatic deposition is smaller than that in the potentiostatic method implying higher efficiency of the galvanostatic method. It was also found that the weight of PANI is reduced by as much as 20% after holding the deposited PANI at a potential below −0.1 V, which suggests that the as-is galvanostatically deposited PANI (G-PANI) is in the doped state with inserted anions. As a result, the measured weight, which includes the weight of both PANI and anions, is greater than the estimated weight. Fig. 4 shows the CV curve of G-PANI on NP-CNFs. The specific capacitance of PANI was computed to be only 350 F g^{-1}_{PANI}. This value is significantly lower than the specific capacitance of PANI deposited potentiostatically (P-PANI), which was unanticipated, since the SEM image (Fig. 5) showed a uniform, thin (50–60 nm), and conformal coating of PANI on the nonporous fibers (NP-CNFs).

A comparison of the CVs of the PANI-coated NP-CNF substrates prepared by the potentiostatic and galvanostatic methods (Fig. 3(a) and Fig. 4) revealed a difference in the shape, indicating difference in the oxidation state of electrodeposited PANI from the two

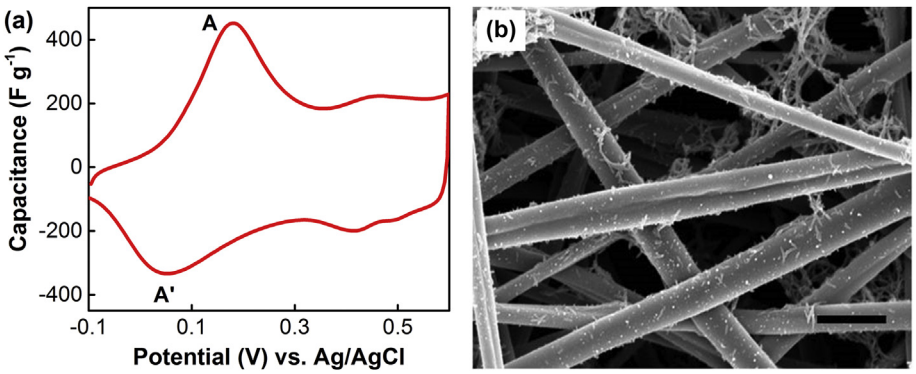

Fig. 3. (a) The cyclic voltammetric response of P-PANI-coated NP-CNF at 20 mV s^{-1}, where PANI was electrodeposited in 0.5 M aniline/1 M H_2SO_4, (b) corresponding SEM image of P-PANI-coated NP-CNF. Scale bar = 1 μm.

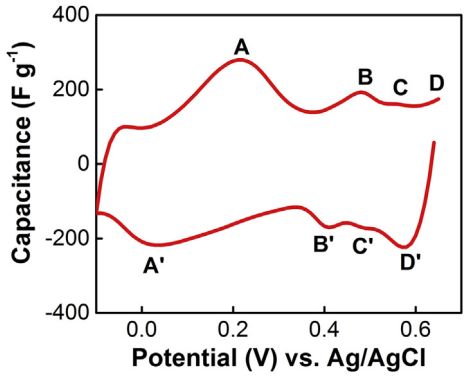

Fig. 4. The cyclic voltammetric response of G-PANI-coated NP-CNF at 20 mV s^{-1}.

techniques. At the lowest potential of −0.1 V, the CV of G-PANI is more rectangular than that of P-PANI. The A′ peak corresponds to the reduced leucoemeraldine, which is an insulating material, and the fact that the CV of G-PANI responds well to the sweeping potential at −0.1 V indicates that some of the PANI is still in the emeraldine salt state, which is highly conductive, suggesting an incomplete reduction at this potential. In order to fully reduce PANI, we expanded the testing negative potential limit to −0.3 V. As seen in Fig. 6, there is a tremendous increase in the intensity of the redox peaks A and A′ corresponding to conversion between LB and ES upon full reduction. The specific capacitance increases to 535 F g_{PANI}^{-1}, and is retained even after switching the lower limit of the potential back to −0.1 V for subsequent cycles. This kind of voltammetric response can be explained by the broad distribution of oxidation states in G-PANI. As a result, a lower potential limit is needed at least for the first cycle to fully reduce these oxidation states. Once complete reduction is achieved, uniform redox peaks are observed within the voltage limit of −0.1–0.7 V. The galvanostatic technique, thus, allows easy control of PANI deposition, with the amount being controlled using the deposition time, and facilitates conformal coating due to precise control over current density (unlike the potentiostatic method). We further investigated this method of deposition of PANI using porous carbon nanofiber (P-CNF) substrates with the aim to achieve even higher capacitance by integrating double-layer capacitance of P-CNFs and pseudocapacitance of PANI. The electrochemical performance of G-PANI-coated P-CNFs (9 mA current for 600 s) at various scan rates is shown in Fig. 7. For comparison, the CV of the uncoated P-CNFs is also included. The first cycle with a lower potential limit of −0.3 V is not shown. The voltammetric curves and specific capacitance remain invariant upon increasing the scan rate to 200 mV s^{-1}, with only a

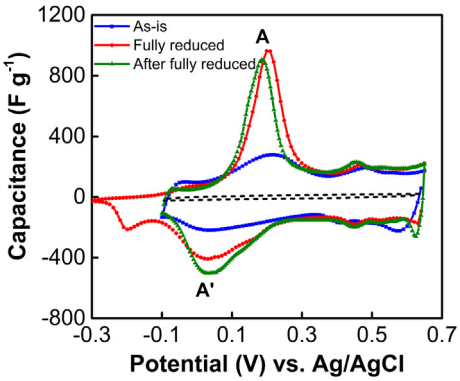

Fig. 6. The cyclic voltammetric response of G-PANI-coated NP-CNFs at 20 mV s^{-1}. Expansion of voltage window down to −0.3 V achieved complete PANI reduction. The dotted curve is for uncoated NP-CNF showing negligible capacitance of the fiber substrate.

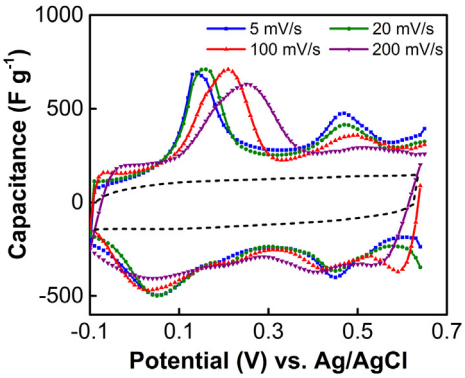

Fig. 7. The cyclic voltammetric response at different scan rates for G-PANI-coated P-CNFs. The dotted curve is for the uncoated P-CNFs at 100 mV s^{-1}.

small shift in peak locations at 200 mV s^{-1} indicating fast kinetics of redox reactions of PANI [2,3], as well as good contact between PANI and carbon substrate. It should also be noted that the rectangular region in the CV scan of PANI-coated P-CNF combines capacitive contributions from both the P-CNF carbon substrate as well as the PANI coating. This suggests that charging and discharging occurs at a pseudo-constant rate over the entire potential window with the PANI contribution arising from both the pseudocapacitance and double-layer capacitance [33,34]. With 38 wt% weight loading of PANI in the tested G-PANI-coated P-CNF sample, specific

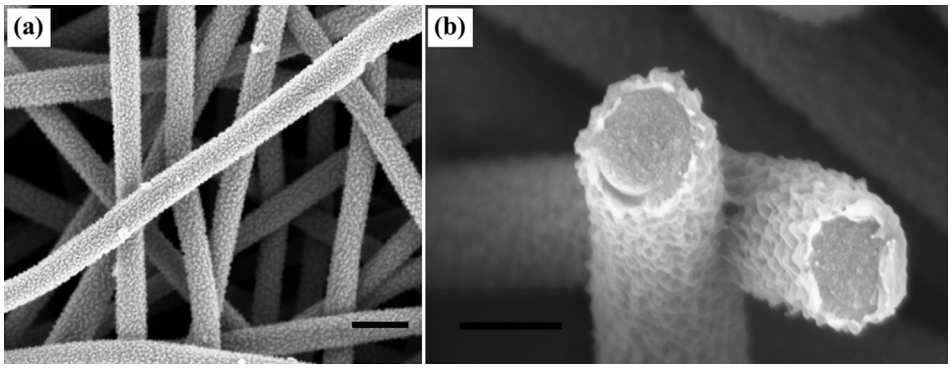

Fig. 5. Scanning electron micrographs of G-PANI-coated NP-CNFs. Scale bars are (a) 1 μm, (b) 500 nm.

Table 1
Values of capacitances after electropolymerization using galvanostatic method.

Sample	PANI wt%	C_{PANI}[a] (F g^{-1}_{PANI})	$C_{PANI/C}$[a] (F $g^{-1}_{PANI/C}$)	$C_{PANI/C}$[a] (F cm^{-3})	$C_{PANI/C}$[a] (F cm^{-2})
PANI on NP-CNFs	43	535	235	78	1.4
PANI on P-CNFs	38	609	320	101	1.5
PANI on P-CNFs	49	600	366	142	1.7

[a] All capacitance values are evaluated at 100 mV s^{-1}.

capacitance of PANI was obtained as 609 F g^{-1}_{PANI}, while the specific capacitance for the composite was 320 F $g^{-1}_{PANI/C}$. A composite specific capacitance of 366 F $g^{-1}_{PANI/C}$ was achieved at a higher PANI loading of 49 wt% at 100 mV s^{-1} scan rate (Table 1). This value is over 2.5 times higher than the specific capacitance of uncoated P-CNFs. Table 1 summarizes the capacitances of the various G-PANI/CNF composites studied in the present work. At a similar loading of PANI, the G-PANI-coated P-CNF composite capacitance is much higher than that of G-PANI-coated NP-CNF sample. This improvement is due to the higher capacitance contribution of P-CNFs (140 F g^{-1}) compared to NP-CNFs (10 F g^{-1}).

The electrochemical performance of the G-PANI-P-CNFs was further investigated by galvanostatic charge–discharge measurements as shown in Fig. 8(a). The charge–discharge curves are quasi-symmetrical due to the redox peaks associated with polyaniline [35]. A high capacitance of 409 F g^{-1} is obtained at a low current density of 0.1 A g^{-1} and 80% of it is retained at 10 A g^{-1}. The specific capacitance data at various current densities for G-PANI-coated P-CNF and NP-CNF along with that of non-coated P-CNF and NP-CNF is provided in Fig. 8(b).

This work demonstrates the fabrication of a true hybrid device integrating electric double layer and pseudocapacitance. Only a few reports have investigated electrodeposition of PANI on carbon fibers. Yang et al. [20] reported vein-like nanostructured PANI on activated CNFs using the potentiodynamic approach. The CV shape was distorted even at a low scan rate indicating high resistance possibly due to larger PANI particle size. Moreover, they did not show any well-defined peaks associated with the transformation between different oxidation states of PANI and the capacitance values dropped off rapidly with increasing current density. Cheng et al. [25] deposited PANI on etched carbon fiber cloth by combining two different techniques: potentiostatic for initial nucleation and galvanostatic for a uniform deposition. They obtained a uniform PANI nanowire coating, which showed a specific capacitance of 673 F g^{-1}_{PANI} and an area-normalized capacitance of 3.5 F cm^{-2}. However, their composite capacitance was only 210 F g^{-1}_{PANI} due to low capacitance contribution from the etched carbon fiber cloth. In the present work, we achieved a composite capacitance of up to 409 F $g^{-1}_{PANI/C}$. Even though our area-normalized capacitance of 1.7 F cm^{-2} (based on CV data at 100 mV s^{-1}) is lower than their report, it can be improved by increasing the thickness of the working electrode or loading of PANI. As a demonstration, we achieved 2.3 F cm^{-2} areal capacitance by slightly increasing the thickness of P-CNFs substrate, without any loss in gravimetric capacitance, owing to the open and interconnected macroporous structure of the nanofiber mats. To test the stability of the G-PANI-deposited samples, 40 wt% G-PANI-coated P-CNF samples were cycled for 1000 cycles at 20 mV s^{-1} scan rate. The composite retained 80% of the initial gravimetric capacitance even after 1000 cycles (Supplementary Fig. S4).

4. Conclusions

The electrodeposition of pseudocapacitive conducting polymer polyaniline on freestanding carbon nanofiber mats was studied. It was found that a significant amount of quinone-like degradation products are formed at low aniline concentration (0.1 M) and high potential limit (1 V) during potentiodynamic electropolymerization/deposition. Increasing aniline concentration to 0.5 M and lowering the potential limit to 0.9 V prevented the formation of degradation products. Both potentiodynamic and potentiostatic methods produced non-uniform, non-conformal, and poor-adhesion coatings of PANI on NP-CNFs. By using galvanostatic electropolymerization method, we achieved a uniform and thin conformal coating of PANI on both NP-CNFs and P-CNFs. At the same loading of PANI, P-CNFs exhibited much higher capacitance than NP-CNFs due to the additional contribution from double layer capacitance of P-CNFs. The combination of two different charge storage mechanisms resulted in excellent specific capacitance of 366 F g^{-1}, 140 F cm^{-3} volumetric capacitance, and up to 2.3 F cm^{-2} areal capacitance in 50/50 (wt/wt) PANI-coated P-CNFs, indicating near-complete retention of carbon double-layer capacitance post

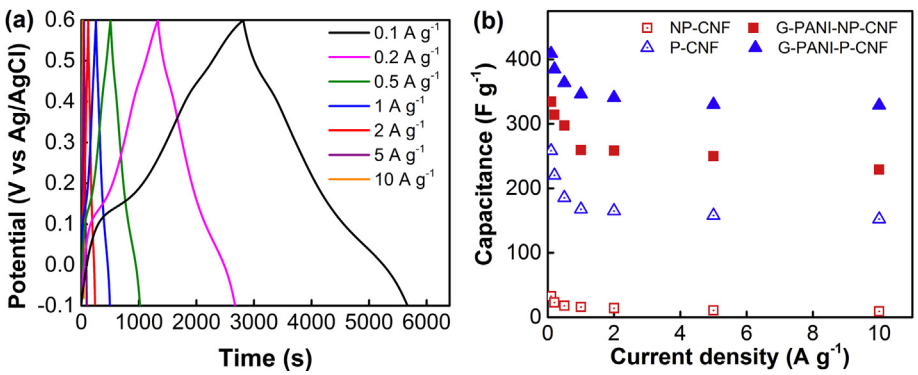

Fig. 8. (a) Galvanostatic charge–discharge curves at various current densities for G-PANI-coated P-CNFs. (b) Specific capacitance data as a function of current density for G-PANI-coated and uncoated P-CNF and NP-CNF.

PANI coating. The thin, conformal coating of PANI reduces the diffusion length of ions during the doping–de-doping process of PANI improving stability and achieving high energy density at high power rate.

Acknowledgments

This work is supported by the National Science Foundation under grant number CAREER CBET-1150528. Authors would like to thank Dr. Jean M. Wallace (Nova Research Inc.) and Dr. Debra Rolison (Naval Research Lab) for their insightful comments and feedback on the manuscript. The authors are grateful to Centralized Research Facility of Drexel University for instrumentation support.

Appendix A. Supplementary data

Supplementary data related to this article can be found at http://dx.doi.org/10.1016/j.jpowsour.2015.05.054.

References

[1] G.A. Snook, P. Kao, A.S. Best, J. Power Sources 196 (2011) 1–12.
[2] Y.G. Wang, H.Q. Li, Y.Y. Xia, Adv. Mater. 18 (2006) 2619–2623.
[3] Y.-Y. Horng, Y.-C. Lu, Y.-K. Hsu, C.-C. Chen, L.-C. Chen, K.-H. Chen, J. Power Sources 195 (2010) 4418–4422.
[4] S. He, X. Hu, S. Chen, H. Hu, M. Hanif, H. Hou, J. Mater. Chem. 22 (2012) 5114–5120.
[5] Y. Zhao, H. Bai, Y. Hu, Y. Li, L. Qu, S. Zhang, G. Shi, J. Mater. Chem. 21 (2011) 13978–13983.
[6] M. Sathish, S. Mitani, T. Tomai, I. Honma, J. Mater. Chem. 21 (2011) 16216–16222.
[7] H.-P. Cong, X.-C. Ren, P. Wang, S.-H. Yu, Energy Environ. Sci. 6 (2013) 1185–1191.
[8] J. Wei, J. Zhang, Y. Liu, G. Xu, Z. Chen, Q. Xu, RSC Adv. 3 (2013) 3957–3962.
[9] G. Yu, X. Xie, L. Pan, Z. Bao, Y. Cui, Nano Energy 2 (2013) 213–234.
[10] X. Yan, Z. Tai, J. Chen, Q. Xue, Nanoscale 3 (2011) 212–216.
[11] Z. Lei, Z. Chen, X.S. Zhao, J. Phys. Chem. C 114 (2010) 19867–19874.
[12] L.L. Zhang, S. Li, J. Zhang, P. Guo, J. Zheng, X.S. Zhao, Chem. Mater. 22 (2010) 1195–1202.
[13] L.Z. Fan, Y.S. Hu, J. Maier, P. Adelhelm, B. Smarsly, M. Antonietti, Adv. Funct. Mater. 17 (2007) 3083–3087.
[14] Y. Li, X. Zhao, P. Yu, Q. Zhang, Langmuir 29 (2013) 493–500.
[15] C. Carlin, L.J. Kepley, A.J. Bard, J. Electrochem. Soc. 132 (1985) 353–359.
[16] S.H. Garlum, J.H. Marshall, J. Electrochem. Soc. 134 (1987) 142–147.
[17] S.-J. Choi, S.-M. Park, J. Electrochem. Soc. 149 (2002) E26–E34.
[18] S.K. Mondal, K.R. Prasad, N. Munichandraiah, Synth. Met. 148 (2005) 275–286.
[19] M.J. Bleda-Martinez, C. Peng, S. Zhang, G.Z. Chen, E. Morallon, D. Cazorla-Amoros, J. Electrochem. Soc. 155 (2008) A672–A678.
[20] J.E. Yang, I. Jang, M. Kim, S.H. Baeck, S. Hwang, S.E. Shim, Electrochim. Acta 111 (2013) 136–143.
[21] H. Zhang, G. Cao, W. Wang, K. Yuan, B. Xu, W. Zhang, J. Cheng, Y. Yang, Electrochim. Acta 54 (2009) 1153–1159.
[22] H. Wei, H. Gu, J. Guo, S. Wei, Z. Guo, J. Electrochem. Soc. 160 (2013) G3038–G3045.
[23] H.-F. Jiang, X.-X. Liu, Electrochim. Acta 55 (2010) 7175–7181.
[24] Y.-Y. Horng, Y.-K. Hsu, A. Ganguly, C.-C. Chen, L.-C. Chen, K.-H. Chen, Electrochem. Commun. 11 (2009) 850–853.
[25] Q. Cheng, J. Tang, J. Ma, H. Zhang, N. Shinya, L.-C. Qin, J. Phys. Chem. C 115 (2011) 23584–23590.
[26] C. Tran, V. Kalra, J. Power Sources 235 (2013) 289–296.
[27] C. Tran, V. Kalra, Soft Matter 9 (2013) 846–852.
[28] D.E. Stilwell, S.-M. Park, J. Electrochem. Soc. 135 (1988) 2254–2262.
[29] H. Yang, A. Bard, J. Electroanal. Chem. 339 (1992) 423–449.
[30] L. Duic, Z. Mandic, S. Kovac, Electrochim. Acta 40 (1995) 1681–1688.
[31] D.-W. Wang, F. Li, Z. Jingping, W. Ren, Z.-G. Chen, J. Tan, Z.-S. Wu, I. Gentle, G.Q. Lu, H.-M. Chen, ACS Nano 3 (2009) 1745–1752.
[32] V. Gupta, N. Miura, J. Power Sources 157 (2006) 616–620.
[33] X. Lang, A. Hirata, T. Fujita, M. Chen, Nat. Nanotechnol. 6 (2011) 232–236.
[34] L. Yang, S. Cheng, Y. Ding, X. Zhu, Z.L. Wang, M. Liu, Nano Lett. 12 (2012) 321–325.
[35] W. Chen, R.B. Rakhi, H.N. Alshareef, J. Mater. Chem. A 1 (2013) 3315–3324.